Capillary waves' dynamics at the nanoscale

2008 J. Phys.: Condens. Matter 20 494229

(http://iopscience.iop.org/0953-8984/20/49/494229)

J. Phys.: Condens. Matter **20** (2008) 494229 (6pp) doi:10.1088/0953-8984/20/49/494229

Capillary waves' dynamics at the nanoscale

Rafael Delgado-Buscalioni[1], **Enrique Chacón**[2] **and Pedro Tarazona**[1]

[1] Departamento Física Teorica de la Materia Condensada, Universidad Autónoma de Madrid, Campus de Cantoblanco, Madrid E-28049, Spain
[2] Instituto de Ciencia de Materiales de Madrid, Consejo Superior de Investigaciones Científicas, Cantoblanco, Madrid E-28049, Spain

E-mail: rafael.delgado@uam.es

Received 31 July 2008, in final form 9 October 2008
Published 12 November 2008
Online at stacks.iop.org/JPhysCM/20/494229

Abstract

We study the dynamics of thermally excited capillary waves (CW) at molecular scales, using molecular dynamics simulations of simple liquid slabs. The analysis is based on the Fourier modes of the liquid surface, constructed via the *intrinsic sampling method* (Chacón and Tarazona 2003 *Phys. Rev. Lett.* **91** 166103). We obtain the time autocorrelation of the Fourier modes to get the frequency and damping rate $\Gamma_d(q)$ of each mode, with wavenumber q. Continuum hydrodynamics predicts $\Gamma(q) \propto q\gamma(q)$ and thus provides a *dynamic measure* of the q-dependent surface tension, $\gamma_d(q)$. The *dynamical* estimation is much more robust than the *structural* prediction based on the amplitude of the Fourier mode, $\gamma_s(q)$. Using the optimal estimation of the intrinsic surface, we obtain quantitative agreement between the structural and dynamic pictures. Quite surprisingly, the hydrodynamic prediction for CW remains valid up to wavelengths of about four molecular diameters. Surface tension hydrodynamics break down at shorter scales, whereby a transition to a molecular diffusion regime is observed.

(Some figures in this article are in colour only in the electronic version)

1. Introduction

The ripples we observe at a liquid surface, on the scale of metres, are dominated by buoyancy forces and are called gravity waves. As one scales down to wavelengths of $\lambda \leqslant 1$ cm, ripples start to be governed by surface tension and become *capillary waves* (CW). The hydrodynamic theory [1–3] for CW still predicts another crossover from the usual propagative (oscillatory) mode to an overdamped non-propagative mode which is set by the balance between the surface tension and the viscous forces. Such crossover has been experimentally observed at $\lambda \sim 0.1$ mm in fluids with low surface tension and large viscosity, such as gels and polymer systems [4], complex fluids [5] and ionic liquids [6]. However, in simple fluids the overdamped hydrodynamic regime is predicted to occur quite close to molecular scales; $\lambda \sim 10\sigma$ in terms of the molecular diameter σ. The validity of the continuum hydrodynamics description at these molecular lengths remains an open question and is one of the main topics of the present work.

Surface tension γ is one of the key parameters in the hydrodynamic description of CW; therefore this question is closely related to the proper determination of the surface tension wavenumber dependence. Experimental and theoretical [7, 8] analysis of thermally excited CW fluctuations in liquid surfaces have to be described in terms of a wavenumber-dependent effective surface tension, $\gamma(q)$, where $q = 2\pi/\lambda$. The deviation of this function from its thermodynamic limit $\gamma(0) = \gamma_o$ is a subject of controversy, with claims of an enhanced CW regime at nanometric scale [7, 9] characterized by $\gamma(q) < \gamma_o$. The experimental evidence [10], and the theoretical basis for that phenomena [8], have been recently criticized, but still the problem of how to measure or calculate $\gamma(q)$ is a crucial question for the analysis of x-ray diffraction experiments on liquid surfaces.

In this work we approach these fundamental questions from molecular dynamic (MD) simulations of simple liquid slabs. We use the *intrinsic sampling method* (ISM) [13, 14] to obtain the instantaneous shape of the intrinsic liquid surface and its associated Fourier modes. As explained in section 2,

the surface modes amplitude leads to a well-known route to measure, from *structural* grounds, the wavenumber-dependent surface tension $\gamma_s(q)$, which however presents significant uncertainties. Here we use the hydrodynamic theory for capillary waves, presented in section 3, to pave a new *dynamic* route to measure the surface tension, $\gamma_q(q)$. Molecular dynamics simulations, depicted in section 4, were used to obtain the surface modes' dynamics (via the ISM method) with excellent agreement with the hydrodynamic predictions. Moreover, as shown in section 5, the best ISM estimation to the intrinsic surface precisely satisfies $\gamma_s(q) = \gamma_d(q)$, hence providing a physically consistent structure *and* hydrodynamics (see also [11]). Using the best ISM estimate for $\gamma_s(q)$, we prove that CW hydrodynamics remain valid up to surprisingly large wavenumbers, $q\sigma \leqslant 2$, well above the validity of the macroscopic surface tension prediction ($q\sigma \leqslant 0.5$). Finally, as demonstrated in section 6, at even smaller scales ($q\sigma \geqslant 2$) surface modes are governed by molecular diffusion, as surface tension hydrodynamics gradually break down. Concluding remarks are given in section 7.

2. The structural determination of the surface tension

In the study of capillary waves at nanoscopic scales, molecular dynamics (MD) simulations can provide a way to connect the molecular structure of the fluid surface and its description as a continuum *intrinsic surface*. The intrinsic surface (IS), usually described in terms of its Fourier components $z = \sum_{\mathbf{q}} \hat{\xi}_{\mathbf{q}} \exp(\mathrm{i}\mathbf{q}\cdot\mathbf{R})$, describes the instantaneous shape of the fluctuating interface, with thermal average parallel to the $\mathbf{R} = (x, y)$ plane. The capillary wave theory (CWT) [12] opens a direct *structural* way to measure the wavevector-dependent surface tension from the mean square amplitude of the CW thermal fluctuations $\langle|\hat{\xi}_q|^2\rangle$ over a transverse area A [13, 14]:

$$\gamma_s(q) = \frac{k_B T}{q^2 \langle|\hat{\xi}_q|^2\rangle A}. \tag{1}$$

However, the CWT considers macroscopic surfaces and it does not provide any procedure to obtain the Fourier components of the IS, $\hat{\xi}_{\mathbf{q}}$, from the molecular structure of the fluid. Indeed, at molecular scales, the intrinsic surface is a *soft* concept, because of the inherent uncertainty of what is the *outermost molecular layer* in a disordered fluid surface. Several methods have been proposed to solve this task in a physically sound way (see [15] for a recent review) and, although the structural approach (1) gives the correct macroscopic limit $\gamma_s(0) = \gamma_o$, for $q\sigma \geqslant 0.5$ the shape of $\gamma_s(q)$ depends on the specific proposal used to measure $\hat{\xi}_{\mathbf{q}}$ from the molecular positions of the fluid [13]. The simplest method, based on a local Gibbs dividing surface, applies thermodynamic arguments to molecular fluid volumes (bins) and therefore it spuriously introduces the effect of mass fluctuations coming from the bulk into the surface description. As a consequence, at large q, it produces an unphysical decay $\gamma_s(q) \sim 1/q^2$ [16]. Recent developments are based on percolation procedures which reconstruct the IS from the local (near-surface) molecular configuration. In this line, Chacón and Tarazona [14, 15] have developed and tested a specific proposal known as the *intrinsic sampling method* (ISM) which solves the problem of determining $\hat{\xi}_{\mathbf{q}}$ through the intuitive concept of the *surface layer*, describing the set of molecules identified as the molecular boundary of the liquid. The method was recently proposed [13] and refined [14] to get the self-consistent identification of the surface layer and the intrinsic surface Fourier components in computer simulations. It has proved to be very useful in extracting the *intrinsic profiles* of the fluid interfaces [15, 17] out of the CW blurred averages. The ISM main input parameter is the surface layer density n_s, which has to be optimized to get the sharpest molecular structure near the interface. Still, n_s, and thus $\gamma_s(q)$, may have significant error bars, particularly as one approaches the critical temperature, and one actually expects to consider the increasing structural disorder of the fluid.

3. Hydrodynamic theory for capillary waves

We now briefly describe the hydrodynamic theory results concerning short wavelength capillary waves. Hydrodynamic analyses, either based on the linearized Navier–Stokes equations [1, 2] or on linear response theory [3], predict the following dispersion relation for surface modes:

$$D(q,\tilde{\omega}) = \frac{\gamma q^3}{\rho} - \left(\tilde{\omega} + 2\mathrm{i}\nu q^2\right)^2 - 2\nu^2 q^4 \left[1 - \frac{\mathrm{i}\tilde{\omega}}{\nu q^2}\right]^{1/2}, \tag{2}$$

where ρ is the liquid density while $\nu = \eta/\rho$ and η are the kinematic and dynamic shear viscosities. The solutions of the characteristic equation $D(q,\tilde{\omega}) = 0$ provide the complex frequencies $\tilde{\omega}(q) = \omega(q) + \mathrm{i}\Gamma(q)$ which rule the temporal behaviour of each surface mode $\hat{\xi}_{\mathbf{q}}(t)$. As the wavenumber is increased, for $q > q_{cr} \sim \gamma\rho/\eta^2$, the dispersion relation (2) furnishes a transition from the usual propagative capillary modes to overdamped waves. Above q_{cr}, the viscous time νq^2 becomes faster than the restoring time of surface tension $(\gamma q^3/\rho)^{1/2}$. As a consequence, the oscillatory part of the complex frequency vanishes, $\omega = 0$, and surface fluctuations are exponentially damped at a rate given by $\Gamma = \mathrm{i}\tilde{\omega}$. Interestingly, in this overdamped regime, the damping rate goes like $\Gamma \sim q\gamma/\eta$ [3]; a relationship which is quite useful for our purposes because it opens a way to evaluate γ from the surface dynamics, i.e. from the damping rate of overdamped surface modes, Γ.

In order to attain the overdamped regime in simple liquids one requires us to consider relatively small wavenumbers $q_{cr}\sigma \sim 0.3$ and therefore one needs to take into account the wavenumber dependence of the transport coefficients. We shall use the q-dependent surface tension provided by the optimum ISM estimate via equation (1). On the other hand, the generalized shear viscosity $\eta(q)$ of the LJ liquid, has been evaluated in several works, either using the generalized hydrodynamics theoretical framework [18, 19] or from non-equilibrium MD simulations [20]. We measured $\eta(q)$ from the liquid velocity response to a sinusoidal spatial forcing and for the LJ fluid we obtained similar values of η/η_o at different temperatures, the best fit being $\eta(q) \simeq \eta_o(1 - 0.079q^2 + 0.011q^3)$.

4. Capillary wave dynamics from MD simulations

Molecular dynamics simulations under periodic boundary conditions were performed to record time series of molecular configurations for each studied case. These configurations were then analysed using the ISM in [14] to obtain the instantaneous intrinsic surface Fourier components $\hat{\xi}_q(t)$ for each allowed wavevector in the periodic box ($\mathbf{q} = 2\pi(\nu_x, \nu_y)/L$, with integer ν_x, ν_y). Molecular dynamics simulations were performed in two different simulation boxes with linear transverse size $L = 9.025\sigma$ and $L = 18.05\sigma$. We prepare the system with a liquid slab of thickness $L_{\rm liq} \approx 3L$, and set much larger periodic conditions on the z direction ($L_z = 90\sigma$ and 120σ, respectively) to get two independent liquid surfaces, separated by a rarefied vapour phase. We have tested that the slab thickness is large enough to avoid the hydrodynamic coupling across the liquid bulk. Simulations were done in the microcanonical ensemble NVE so as to ensure local momentum conservation and proper hydrodynamics. However, we obtained similar results in the isothermal (NVT) ensemble, assuming a thermostat with large enough inertial time (the limit being the slowest CW within the box). The time step was $\Delta t = 0.005\tau$ (with $\tau \equiv \sigma(\epsilon/m)^{1/2}$ the usual LJ time unit) and configurations were sampled each $\Delta t_{\rm samp} = 0.05\tau$ or 0.5τ, depending on the CW timescale to be analysed. The ISM was used in post-processing to obtain $\hat{\xi}_q(t)$.

In order to validate the hydrodynamic theory summarized in equation (2), under our molecular set-up we decided to observe the propagative–overdamped transition. To that end, we considered a fluid model with a very stiff surface, thus providing a large crossover wavenumber $q_{\rm cr} \sim \gamma\rho/\eta^2$. At a temperature $kT = 0.212\epsilon$, the *soft-alkali* (SA) cold-liquid model [21] yields $q_{\rm cr} = 0.8/\sigma$ and permits us to observe the transition using manageable MD boxes of transverse size $L \approx 20\sigma$. In order to extract the angular frequency $\omega_{\rm d}$ and the damping rate $\Gamma_{\rm d}$ of each mode we fitted the autocorrelation (ACF) function $\langle\hat{\xi}_q(t)\hat{\xi}^*_q(0)\rangle$ to $\langle|\hat{\xi}_q|^2\rangle \exp(-\Gamma_{\rm d}t)\cos(\omega_{\rm d}t)$. Results are shown in figure 1. The corresponding macroscopic hydrodynamic predictions Γ_o and ω_o (obtained by inserting the macroscopic surface tension γ_o and viscosity η_o in the dispersion relation (2)) are indicated with dashed lines in figure 1, while the use of our best ISM estimate for $\gamma_{\rm s}(q)$ into equation (2) leads to $\Gamma_{\rm s}$ and $\omega_{\rm s}$, shown as full lines. Hydrodynamic predictions correctly forecast the oscillatory branch and the transition to the overdamped regime obtained in MD simulations, thus confirming the validity of equation (2) in the present context. In the case of the SA liquid the macroscopic Γ_o and q-dependent solution $\Gamma_{\rm s}$ remain quite similar up to $q\sigma < 1.5$. However, as shown soon below, this is due to the peculiar properties of the SA liquid, whose transport properties show little dependence on the wavenumber: $\gamma_{\rm s}(q) \simeq \gamma_o$ up to $q\sigma \leqslant 1.0$, while the viscosity $\eta(q) \simeq \eta_o$ for $q\sigma \leqslant 1.5$.

We now focus on more typical liquids with much higher triple point temperature than the SA model, to analyse the surface behaviour at larger q within the strong damping regime. To avoid freezing, one has to work at higher temperatures, meaning lower surface tension, and hence smaller crossover

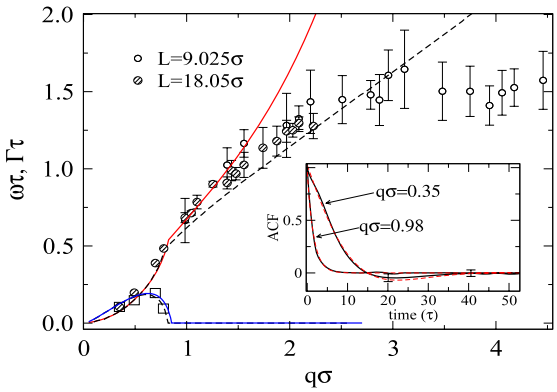

Figure 1. The decay rate Γ and angular frequency ω wavenumber dependence of capillary modes in a soft-alkali (SA) liquid model at $T = 0.212\epsilon/k$, density $\rho = 1.17\sigma^{-3}$, surface tension $\gamma_o\sigma^2/(kT) \approx 8.23$ and shear viscosity $\eta = 1.5\epsilon\tau/\sigma^3$. Symbols correspond to $\Gamma_{\rm d}$ (circles) and $\omega_{\rm d}$ (squares) obtained from MD simulations of different box transversal sizes L. Lines are the hydrodynamic predictions, using $\gamma_{\rm s}(q)$ (solid line) and γ_o (dashed line). Standard Lennard-Jones units are used throughout: here $\tau = \sigma(\epsilon/m)^{1/2}$. The inset show normalized ACF (solid line) and fitting functions (dashed lines) for a propagating ($q\sigma = 0.35$) and one overdamped ($q\sigma = 0.98$) mode.

wavenumber. The results obtained for the Lennard-Jones (LJ) liquid presented in figure 2 correspond to $q_{\rm cr}\sigma = 0.32$, so the entire range of q allowed in our simulation box (size $L = 10.46\sigma$) is now within the overdamped regime. In this case, the damping rate $\Gamma_{\rm d}$, directly extracted from the exponential decay of the ACF, starts to deviate from the macroscopic hydrodynamic prediction Γ_o above $q\sigma \geqslant 0.5$ and, around $q\sigma \simeq 2$, $\Gamma_{\rm d}$ becomes five times larger than Γ_o. This large underestimation of the macroscopic limit Γ_o is observed at all the temperatures considered.

In order to understand such large discrepancy one needs to consider the values of $\gamma_{\rm s}(q)$ extracted from equation (1). As shown in figure 2, the damping rate $\Gamma_{\rm s}$ obtained by insertion of the optimal ISM estimate $\gamma_{\rm s}(q)$ and $\eta(q)$ into the hydrodynamic relation arising from equation (2) extends the agreement with the exponential decay of the ACF Γ_q, up to $q\sigma \leqslant 2$. It is most remarkable that the continuous hydrodynamic description of the surface fluctuations may be valid down to a wavelength of about three or four molecular diameters, with the use of an independently obtained function $\gamma_{\rm s}(q)$. Such agreement is kept at other temperatures in the LJ fluid and also in the cold-liquid SA model (up to $q\sigma \leqslant 1.5$, see figure 1). Figure 2(b) shows results for the LJ fluid at another temperature, $kT = 0.848\epsilon$, plotted against the wavelength $\lambda = 2\pi/q$, to clearly illustrate the range of validity of the (generalized) hydrodynamic trend $\Gamma_{\rm s}$. These results are strong evidence for the validity of the hydrodynamic description of CW fluctuations at the nanoscale [3, 1, 2], and they also validate the ISM used to get the IS shape from the atomic positions. However, in order to finally prove these claims, one still needs to analyse to what extent do the values of $\Gamma_{\rm s}$ and, in particular $\Gamma_{\rm d}$, depend on the detailed procedure to get $\hat{\xi}_{\mathbf{q}}$ from the molecular positions.

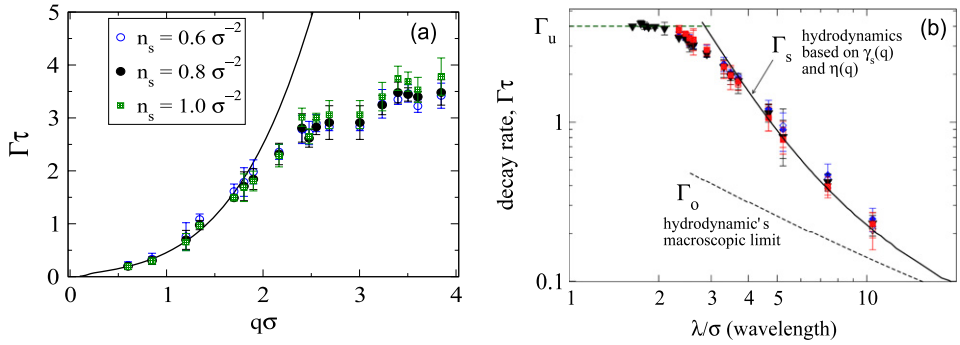

Figure 2. The decay rate Γ of CWs in a Lennard-Jones liquid at (a) $T = 0.763\epsilon/k$, density $\rho = 0.782\sigma^{-3}$, viscosity $\eta_o = 1.85\,\epsilon\tau/\sigma^3$ and surface tension $\gamma_o\sigma^2/(kT) = 0.93$ and at (b) $kT = 0.848\epsilon$, $\rho = 0.738\sigma^{-3}$, $\eta_o = 1.5\epsilon\tau/\sigma^3$ and $\gamma_o\sigma^2/(kT) = 0.653$. Symbols are obtained from MD simulations by fitting the surface mode ACF obtained for several surface density parameters n_s to $\langle|\hat{\xi}_q|^2\rangle \exp(-\Gamma_d t)$. The solid line corresponds to the hydrodynamic prediction using the optimal $\gamma_s(q)$ (at (a) $n_s = (0.75 \pm 0.05)\sigma^{-2}$ and (b) 0.70 ± 0.05). The dashed line is the macroscopic trend, using γ_o and η_o.

5. A dynamic route to the surface tension

As stated in section 2, the determination of $\gamma_s(q)$ from the ISM values for $\langle|\hat{\xi}_q|^2\rangle$ and equation (1) is a rather delicate matter. The ISM result depends on the surface layer density n_s, which is the main control parameter of the method, and it has to be optimized to get the sharpest view of the molecular layering [14]. The results for atomic, molecular and metallic fluids have shown that the optimal n_s can be satisfactorily determined and that it contains physically relevant information on the interfacial structure, but still has relatively large error bars, particularly as one increases the temperature towards the critical one, $T = T_c$. For instance, in the case of the LJ liquid at $kT = 0.933\epsilon$ ($T/T_c = 0.77$), the optimal choice [14] is to take $n_s = 0.65 \pm 0.05$ atoms per σ^2 area. The dashed lines in figure 3 show that the resulting $\gamma_s(q)$ greatly varies as one changes the surface layer density parameter between $n_s = 0.5/\sigma^2$ and $n_s = 1.0/\sigma^2$. We stress that, for the same atomic configuration, the choice of the n_s parameter leads to a different IS shape. This issue is rather important because if the surface dynamics were also to depend on the choice of n_s, then it will not be clear how to get a precise definition of the intrinsic surface.

Luckily, as illustrated in figure 2, the value of Γ_d extracted from the time ACF of the surface modes is very insensitive to the value of n_s. This is probably due to the fact that the hydrodynamic collective behaviour of the atoms *nearby* the surface is more robust than its intrinsic structure, which depends to a greater extent on the *precise* location of the atomic positions. The result in figure 2 indicates that it is possible to obtain a parameter-independent *dynamical* measure of the q-dependent surface tension, $\gamma_d(q)$. Such evaluation is done via the numerical inversion of the hydrodynamic relation for the damping rate $\Gamma = i\tilde{\omega}(q; \gamma, \eta)$ (arising from $D(q, \tilde{\omega}) = 0$ in equation (2)). The results illustrated in figure 3 confirm our expectation and enable us to conclude two important points.

(i) The dynamic prediction $\gamma_d(q)$ is practically independent of the first liquid layer density n_s, in clear contrast with the structural one, $\gamma_s(q)$.

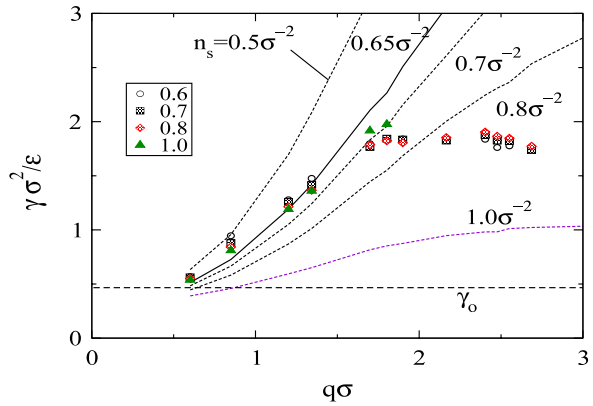

Figure 3. The surface tension γ of a Lennard-Jones liquid at $T = 0.933\epsilon/k$, density $\rho = 0.688\sigma^{-3}$, $\eta_o = 1.18\epsilon\tau/\sigma^3$ and $\gamma\sigma^2/(kT) = 0.5$. Values of γ_d (symbols) come from the numerical inversion of the hydrodynamic relation $\Gamma_d = \Gamma(q, \gamma_d, \eta)$ at the MD decay rate Γ_d. Lines correspond to the ISM structural predictions, equation (1). Results for values of the first layer density n_s are compared. The optimal n_s predicted by the structural analysis $n_s = (0.65 \pm 0.05)\sigma^{-2}$, is indicated with the solid line.

(ii) The surface tension $\gamma_s(q)$ obtained for the optimal surface density n_s is the only structural estimation which coincides with the dynamical one: $\gamma_s(q) = \gamma_d(q)$.

As stated, the optimal n_s furnishes the intrinsic surface, providing the sharpest view of the intrinsic density profile [14]. This fact highlights the relevance of the second conclusion (ii) as it supports the existence of an intrinsic surface definition which consistently links the structural and dynamical roles of the surface tension.

6. Beyond the hydrodynamic regime: molecular diffusion

As shown in figures 1 and 2, above a certain wavenumber $q > q_u$, the damping rate Γ_d obtained from $\langle\xi_q(t)\xi_q(0)\rangle$ gradually deviates from the hydrodynamic trend and saturates to a constant (q-independent) value, Γ_u. This limiting

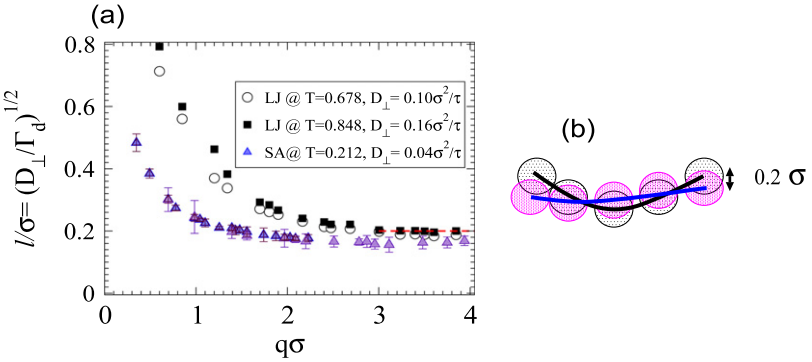

Figure 4. The distance ℓ travelled by a molecule by diffusion in a normal-to-surface direction, over the decorrelation time $1/\Gamma_d(q)$, against the wavenumber q. For $q\sigma > 2$, ℓ converges to a constant value $\ell \simeq 0.2\sigma$ which is almost independent of the fluid considered. (b) An example of two decorrelated configurations of a mode with wavelength $\lambda = 4\sigma$, which differ by an average molecular displacement of 0.2σ.

damping rate of modes with very short wavelength is also illustrated in figure 2(b). Both q_u and Γ_u depend on the liquid considered and typically $q_u\sigma \in [1.5\text{–}2.0]$. It is surprising the hydrodynamic regime reaches so far within the nanometric scale but what is the physical origin of the timescale Γ_u^{-1} arising at even shorter wavelengths? These nanometre 'waves', with $\lambda \leqslant 4\sigma$, involve very few surface molecules, softly linked together by interatomic forces. Their decorrelation time Γ_u^{-1} should then be of the same order as the diffusion time required for one molecule to move a small (molecular) distance ℓ in the out-of-plane direction. Following this argument we define $\ell \sim \sqrt{D_\perp/\Gamma_d}$, where $D_\perp$ is the local coefficient for out-of-plane molecular diffusion, recently calculated in [22] via a Smoluchovsky-type equation to fit the spatiotemporal distribution of molecules nearby the intrinsic surface. Figure 4(a) shows how ℓ depends on the wavenumber for the LJ fluid at different temperatures and the cold SA model. Values of $D_\perp$ from [22] are indicated in the legend. Interestingly enough, ℓ converges to a constant value at large q: we get $\ell = (0.19 \pm 0.01)\sigma$ for all the LJ cases considered and $\ell = (0.18 \pm 0.01)\sigma$ for the SA case. Such a nice agreement indicates that the surface dynamics at $q > q_u$ are governed by single molecule diffusion. In any case, the crossover from surface-tension-driven CWs to (Brownian) diffusive motion is gradual, as molecular diffusion becomes the slowest 'mode' (i.e. for $\Gamma(q) > D_\perp/\ell^2$). The small value of the decorrelation distance ($\ell \simeq 0.2\sigma$) seems to arise from a general feature, related to geometrical aspects of the molecular arrangement. In fact, figure 4(b) illustrates that it is quite possible to obtain two decorrelated configurations of a mode with $\lambda = 4\sigma$, by displacing the (spherical) particles a fraction of its radius. Following the clues in [22], it is possible to provide a finer connection with surface structure dynamics. The value of the 'decorrelation length' deduced here ($\ell \simeq 0.2\sigma$) agrees with the so-called 'split' displacement Δx_s defined in [22]. The value of Δx_s is the molecular mean square displacement (MSD) above which in-plane displacement ($\text{MSD}_\parallel$) becomes larger than out-of-plane displacement ($\text{MSD}_\perp$). Note that $\text{MDS}_\perp$ has to saturate to reach the width of the surface $[\sum_q \langle|\hat{\xi}_q|^2\rangle]^{1/2}$, while $\text{MSD}_\parallel$ grows following a classic diffusion law. Therefore, the 'split' time $t_s \equiv \Delta x_s^2/D_\perp$ after which $\text{MSD}_\parallel > \text{MSD}_\perp$, is also the time required for an instantaneous surface molecular configuration to decorrelate to a new one, i.e. $\Gamma_u \simeq 1/t_s$. Or, in other words, the typical time needed to pass from two configurations similar to those illustrated in figure 4(b).

7. Concluding remarks

To conclude, we have shown that capillary waves in simple liquids are governed by hydrodynamics up to nanometric scales, while molecular diffusion becomes the dominant mode for wavelengths below a few particle diameters. In the hydrodynamic regime, the estimation of the surface tension based on its dynamic role $\gamma_d(d)$ is quite robust with respect to the detailed definition of the intrinsic surface. The *optimal* surface predicted by the implicit sampling method [14, 15] provides physically consistent structural and dynamical definitions, i.e. $\gamma_s(q) = \gamma_d(q)$. Finally, the monotonic increase of $\gamma(q)$ disclaims the existence of an enhanced CW regime [9] that would imply a decrease of the surface tension (and damping rate) below the macroscopic prediction.

The robust character of the collective dynamics near a simple liquid surface, as observed in this work, opens up the challenge to extend the ISM to other interesting scenarios. In particular those involving significant surface fluctuations, like simple liquids near the critical region, and the surface of viscoelastic or complex fluids, such as polymer–colloid mixtures with very low surface tension. These complex mixtures exhibit exotic phenomena such as the possibility of suppressing thermally excited capillary waves by shear flows [23], which may also be considered in other fluids.

Acknowledgments

The authors acknowledge fruitful discussions with D Duque. This work is supported by the Dirección General de Investigación of Spain under grant FIS2007-65869-C03 and by the Comunidad Autónoma de Madrid under grant s-0505/ESP-0299. RD-B benefits from the Spanish Ministerio de Educación y Ciencia 'Ramon y Cajal' research contract.

References

[1] Harden J, Pleiner H and Pincus P A 1991 *J. Chem. Phys.* **94** 5208
[2] Jeng U-S *et al* 1998 *J. Phys.: Condens. Matter* **10** 4955
[3] Jäckle J and Kawasaki K 1995 *J. Phys.: Condens. Matter* **7** 4351
[4] Dorshow R B and Turkevich L A 1993 *Phys. Rev. Lett.* **70** 2439
Kikuchi H *et al* 1994 *Phys. Rev.* B **49** 3061
[5] Madsen A *et al* 2004 *Phys. Rev. Lett.* **92** 096104
[6] Sloutskin E *et al* 2008 *Phys. Rev.* E **77** 060601(R)
[7] Mecke K and Dietrich S 1999 *Phys. Rev.* E **59** 6766
[8] Tarazona P *et al* 2007 *Phys. Rev. Lett.* **99** 196101
[9] Fradin C *et al* 2000 *Nature* **403** 6777
Mora S *et al* 2003 *Phys. Rev. Lett.* **90** 216101
[10] Pershan P 2000 *Colloids Surf.* A **171** 149
Shpyrko O *et al* 2004 *Phys. Rev.* B **69** 245423
[11] Delgado-Buscalioni R, Chacón E and Tarazona P 2008 *Phys. Rev. Lett.* **101** 106102
[12] Buff F *et al* 1965 *Phys. Rev. Lett.* **15** 621
[13] Chacón E and Tarazona P 2003 *Phys. Rev. Lett.* **91** 166103
Chacón E and Tarazona P 2004 *Phys. Rev.* B **70** 235407
[14] Chacón E and Tarazona P 2005 *J. Phys.: Condens. Matter* **17** S3493
[15] Bresme F *et al* 2008 *Phys. Chem. Chem. Phys.* **10** 4704
[16] Stecki J 1998 *J. Chem. Phys.* **109** 5002
Werner A *et al* 1999 *Phys. Rev.* E **59** 728
[17] Chacon E *et al* 2006 *Phys. Rev.* B **74** 224201
Chacon E *et al* 2006 *J. Chem. Phys.* **125** 014709
[18] Mryglod I M and Omelyan I P 1997 *Mol. Phys.* **92** 913
[19] Boon J P and Yip S 1992 *Molecular Hydrodynamics* (New York: Dover)
[20] Ciccotti G, Jacucci G and McDonald I R 1975 *Phys. Rev.* A **13** 426
[21] Chacon E *et al* 2001 *Phys. Rev. Lett.* **87** 166101
Velasco E *et al* 2002 *J. Chem. Phys.* **117** 10777
[22] Duque D *et al* 2008 *J. Chem. Phys.* **128** 134704
[23] Derks D *et al* 2006 *Phys. Rev. Lett.* **97** 038301
See also, Jamie E A G *et al* 2008 *J. Phys.: Condens. Matter* **20** 494231